X-Ray Imaging of Desiccation Cracking Patterns in Geosynthetic Clay Liners

J.J. Potvin and W.A. Take
Department of Civil Engineering– Queen's University, Kingston, ON, Canada
G.A. Siemens
Department of Civil Engineering– Royal Military College of Canada, Kingston, ON, Canada
A. Kerr
Cancer Centre of Southeastern Ontario, Kingston, ON, Canada

ABSTRACT
A geosynthetic clay liner (GCL) is a low permeability layer that is often used as part of a composite liner in various hydraulic barrier applications, such as landfills. The GCL consists of bentonite, a high swelling clay, that is bonded to other geosynthetic layers by needle punched fibres or epoxy. After placement of the liner on a foundation soil, the bentonite must hydrate by absorbing water from the subsoil in order to achieve a homogeneous structure and its low hydraulic conductivity. However, if these GCLs subsequently lose moisture, the internal bentonite layer is susceptible to cracking due to an increase in matric suction. As long as the swelling properties of bentonite remain intact, these cracks have the potential to heal upon rehydration and the GCL will regain its low hydraulic conductivity. To investigate this cracking process, a sample of GCL was slowly dried to known target moisture contents and the sample was interrogated non-invasively for cracks using digital x-ray imaging technology. This paper describes the image processing techniques developed to quantify cracks in GCLs and provides preliminary findings on the cracking patterns of an 'off the roll' liner.

RÉSUMÉ
Une géocomposite bentonitiques (GCB) est une couche à faible perméabilité qui est fréquemment utilisée comme revêtement composite dans des applications variées des barrières hydrauliques, telles que les décharges. La GCB est composée de bentonite, une argile gonflante. Grâce à une méthode aiguilletée ou d'époxy, celle-ci est liée à d'autres couches de fibres géosynthétiques. Après le placement de la chemise géosynthétique sur un sol de fondation, la bentonite doit imprégner l'eau. Pour ce faire, elle absorbe l'eau du sous-sol, ce qui lui permet de parvenir à sa structure massive ainsi qu'à sa faible conductivité hydraulique. Toutefois, si ces GCB perdent de l'humidité, la couche de bentonite interne est sensible à la fissuration due à une augmentation de la succion matricielle. Si les propriétés de gonflement de la bentonite ne sont pas affectées et donc, demeurent malgré tout intacts, ces fissures générées par la perte d'humidité ont le potentiel de se régénérer lors de la réhydratation. Cela dit, la GCB retrouvera sa faible conductivité hydraulique. Afin d'étudier ce procédé de craquage, un échantillon de GCB a séché lentement jusqu'à l'atteinte de la teneur en eau ciblée. Cet échantillon fut examiné de façon non destructive des fissures en utilisant la technologie numérique d'imagerie à rayons X. Cet article traitera des techniques de traitement d'images mis au point dans l'objectif de quantifier les fissures dans les GCB et fournit, entre autres, des résultats préliminaires sur les habitudes de la fissuration d'une couche qui provient d'un rouleau du manufacturier.

1 INTRODUCTION

A geosynthetic clay liner (GCL) is a low permeability liner that is commonly used in various hydraulic barrier applications, such as landfills. In a GCL, a highly swelling clay (bentonite) is bonded to geosynthetic layers with either needle punched fibres or epoxy. When installed on the foundation soil, the GCL must uptake moisture from the subsoil in order to form its massive structure and achieve its low hydraulic conductivity. In typical landfill liner applications, it is common for a geomembrane liner to be placed on top of the GCL to form a composite liner system. If this geomembrane is left exposed to solar radiation for extended periods of time, the large daily changes in liner temperature can result in a reduction of the GCL's moisture content. This reduction in moisture content has the potential to induce shrinkage strains within the GCL (e.g. Thiel and Richardson, 2005; Koerner and Koerner, 2005, Bostwick et al, 2010; Rowe et al., 2011) and has been observed to cause desiccation cracking (e.g. Take et al., 2009). If cation exchange does not occur, GCLs that have experienced desiccation cracking are capable of self healing upon rehydration with foundation soil pore water and can regain its low hydraulic conductivity (e.g. Boardman and Daniel, 1996). However, if the swelling index of the GCL are reduced due to cation exchange, the hydraulic conductivity of a rehydrated sample can be up to three orders of magnitude larger than the original value (Albrecht and Benson, 2001).

X-ray imaging has been shown by Take et al. (2009) to be a non destructive imaging technique in order to identify crack patterns that develop in GCL's upon shrinkage. During imaging, the difference in x-ray intensities that reach the detector are measured and displayed as a grayscale picture. The imager is calibrated

so that the unattenuated x-rays have zero amplitude (black) whereas the attenuated x-rays have a non-zero image amplitude (gray to white). Thus, for a desiccated GCL, cracks in the liner appear dark and the bentonite solids will be a grayish-white colour. The attenuation along any rayline is dependent on the number of atoms available for photon interaction. More atoms are present as the thickness and density of the object is increased, thus increasing the probability of an x-ray photon interaction (Huda, 2003). However, the bentonite in GCLs have both a thin structure (e.g. 1 cm thick) and a relatively low material density. Consequently, attenuation becomes an issue since the contrast between cracks and the bentonite region is very low. This has the implication that careful attention to error sources in the x-ray images is needed to effectively analyse the cracking behaviour of GCLs during desiccation. The objective of this paper is to develop the imaging techniques required to enable a direct comparison of x-rays taken at various time intervals to quantify the evolution of crack patterns in GCLs.

2 MATERIALS AND METHODS

The material selected to investigate x-ray imaging techniques was a non-thermally treated needle punched GCL product which contains a coarse granular bentonite sandwiched between a nonwoven cover and carrier geotextile. This GCL type was chosen for analysis as it is a commonly used product in North America and is one of the products currently being studied (GCL4) in the wider research program of GCL behaviour at Queen's University (e.g. Beddoe et al., 2010; Beddoe et al., 2011; Bostwick et al., 2010; and Brachman et al., 2007).

Desiccation cracking was induced in the GCL by first initially hydrating each specimen to reach full saturation before subjecting it to gradual step-wise air drying episodes. The GCL was initially hydrated for two weeks in a temperature control room (20°C +/- 0.5°C) by submerging in distilled water while applying a 2 kPa normal stress. After hydration, the GCL was then removed from the saturation bin and the cover and carrier geotextile were lightly dabbed with a paper towel to remove excess moisture. A moisture barrier tape (e.g. tuck tape) was then placed on the GCL as shown in Figure 1. The insulation tape was shown by Beddoe at al. (2010) to reduce the moisture content variations in GCL specimens due to preferential drying of GCL samples at the edges. Also shown in Figure 1 are four metal washers affixed to the cover geotextile with epoxy (LePage Epoxy Gel). It is difficult to place the GCL samples in the same frame of reference at each imaging session, thus the highly attenuating washers provide an accurate and consistent coordinate system that appear clearly in both the x-ray and optical images. As a result, these washers enable the images to be corrected for changes in the orientation of the GCL sample on the x-ray imager between imaging sessions.

Air drying of the GCL was accomplished by placing GCL samples on an elevated geonet rack that permitted loss of moisture through the cover and carrier geotextiles of the GCL for short periods of time until target moisture contents were reached. The GCL specimens were then immediately removed from the rack and placed into two double locking freezer bags to minimize moisture loss and stored for a minimum of 24 hours prior to imaging.

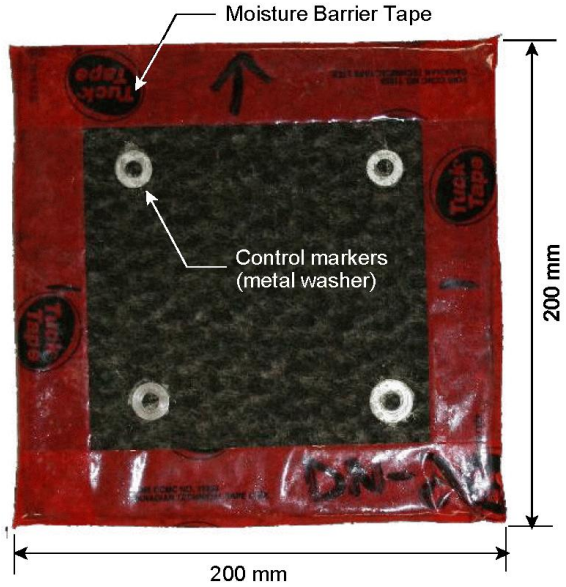

Figure 1. Digital photograph of GCL specimen showing moisture barrier tape and washer control markers.

At the end of each drying step the specimen was photographed using both a SLR digital camera and an x-ray imager. The photographic images were acquired using a 10 megapixel Digital Rebel XTi SLR camera at a constant focal length of 28mm. At 3888 x 2592 pixels the pixel size corresponds to approximately 0.22 mm at the sample plane. Images taken at the initial moisture content of 198% and at lower target moisture contents of 124% and 9.6% are presented in Figure 2. These images show that the moisture barrier tape in both of the planar dimensions of the GCL have experienced shrinkage.

The x-ray images were captured using a kilovolt (kV) x-ray imager at the Cancer Centre of Southeastern Ontario. GCL specimens were x-rayed at 65 kV with a 400 x 300 mm imaging panel placed 1.19 m from the radiation source. The GCLs were placed directly on the imaging panel, therefore at 2048 x 1536 pixels; the pixel width at the sample plane was 0.194 mm.

3 SHRINKAGE STRAINS

Throughout drying, strains are developed in the GCL and are recorded at the end of every drying episode by measuring the change in distance between the horizontal and vertical washers using digital calipers. The strain patterns that developed in the GCL are due to the shrinkage of the bentonite core. These strains may be affected by the properties of the cover and carrier geotextiles, variations in anchorage provided by needle punching fibres between product types, the uniformity of bentonite distribution and the variability in product properties related to the roll location from which the sample was cut (Bostwick et al. 2010; Rowe et al., 2011). Because these factors affect the strain in the GCL it is

possible that these factors also influence the crack pattern developed in GCLs.

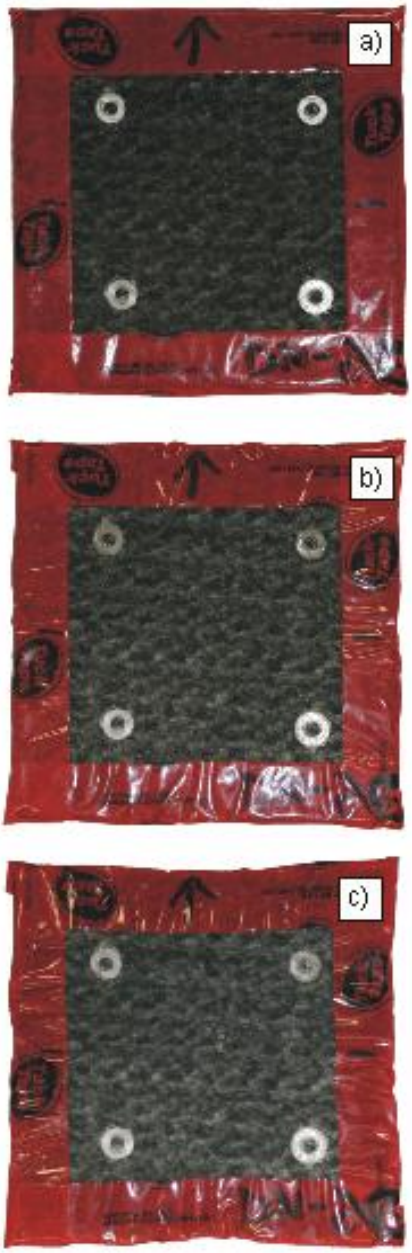

Figure 2. Digital images of the GCL specimen at gravimetric water contents of a) 198% b) 124.3% and c) 9.6%.

Defining shrinkage strain as zero in the initial hydrated GCL, the measurements of washer position were used to calculate the strains in the GCL sample during drying. As shown in Figure 3, the strains in the longitudinal (roll) direction were larger than in the transverse (cross-roll) direction and strains increased with the level of moisture content loss. The observed anisotropy in shrinkage strain is consistent with the observations of Bostwick et al., 2010 who observed that GCL samples preferentially shrink in the longitudinal direction. The GCL reached a maximum strain in the longitudinal and transverse direction of approximately 11% and 7% respectively.

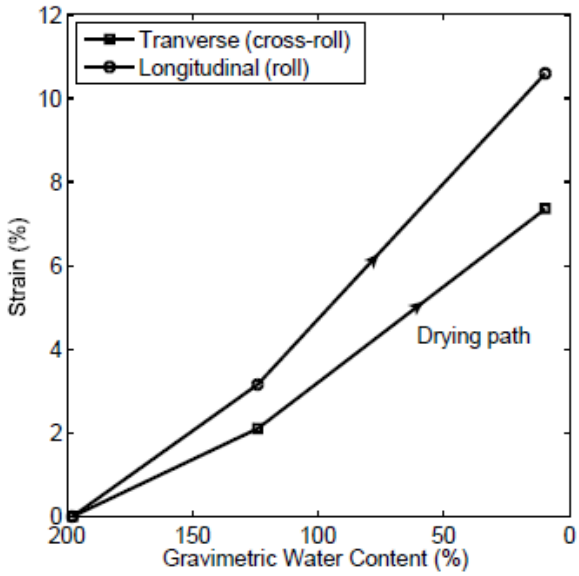

Figure 3. Strains observed in the GCL specimen upon drying

4 IMAGE CORRECTION TECHNIQUES

In order to effectively analyse and quantify the cracking patterns developed in GCLs, imaging correction techniques are required to ensure the contrast between the cracks and the bentonite region is both measurable and reproducible. To meet the objective, a further investigation of a) the consistency of the x-ray formation process and b) the attenuation contrast of GCLs is required. This investigation is completed by the use of two phantoms; a (50.1 x 112.29 x 10.36 mm thick) bentonite phantom constructed by mixing bentonite particles with epoxy gel, and a commercial high resolution medical image quality test phantom (Standard Imaging Inc, 2011).

4.1 Image Correction Using Bentonite Phantom

The bentonite phantom was formed by mixing bentonite clay that had been collected from a GCL sample with LePlage Expoy Gel. Figure 4 shows a photograph and x-ray image of the bentonite phantom. The purpose of the epoxy is to mould the bentonite particles together and act as a substitute for water since the density of the epoxy and water are approximately equal. The bentonite/epoxy mixture was created in a mould and compressed to match the properties of a GCL that is approximately at a moisture content of 115% (i.e. an epoxy content of 115% by mass). The thickness of a GCL upon swelling varies between products; the typical height can range from 10 to 12 mm when fully hydrated, thus the bar thickness was designed within this range. As a result of these dimensions and the epoxy to bentonite ratio, the density was designed to be 1.3 g/cm^3.

A series of grooves were machine-cut into the bentonite phantom with dimensions shown in Table 1. The machined grooves were intended to simulate typical desiccation cracks of varying size that can form in a GCL. The width, depth and spacing between cracks were varied in order to observe the change in contrast between cracked and solid bentonite. From this analysis it is evident that there is sufficient image contrast for all grooves down to a crack width of 0.75mm, except when the depth is shallow (1.0 mm). This inability to measure shallow cracks is not significant in this study as post mortem examinations of cracked GCLs indicate once formed, cracks propagate through the full thickness of the GCL due to the small thickness of the bentonite core.

4.2 Image Correction Using QCKV-1 (Bar) Phantom

To ensure that the x-ray imaging technique had sufficient contrast to distinguish between cracks and solid bentonite x-ray imaging of a commercial phantom was undertaken. The QCKV-1 Phantom was used with a therapeutic kV imager in order to ensure the imager is performing optimally and producing quality images. The phantom provides quantitative information regarding resolution, contrast-to-noise values and overall noise (Standard Imaging Inc, 2011).

The commercial phantom is displayed as a a) photographic image and b) x-ray image in Figure 5. It is a 0.25 kg rectangular bar with outer dimensions of 10.7 cm x 12.7 cm x 1.6 cm. The phantom is organised into 15 different regions as shown in the visual image. Regions 1 to 5 are the line-pairs with bar resolution and thicknesses outlined in Table 2. Regions 6 to 11 consist of 5 different contrast level region in which each section allows for a specific transmission rate as seen in Table 2. The four corner regions are contrast details that are used to determine the level of contrast when the phantom is imaged.

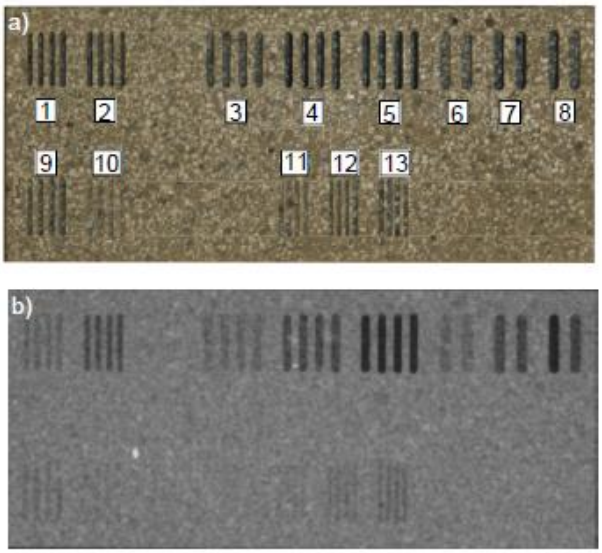

Figure 4. a) Optical and b) x-ray image of the bentonite Phantom with various machine cut groves to test image resolution (Note: properties of the numbered groves are outlined in Table 1).

Table 1. Bentonite Phantom Groove Properties

Number	Width (mm)	Depth (mm)	Spacing (mm)
1	1.0	3.0	2.0
2	1.0	6.0	2.0
3	1.5	3.0	3.0
4	1.5	6.0	3.0
5	1.5	9.0	3.0
6	2.0	3.0	4.0
7	2.0	6.0	4.0
8	2.0	9.0	4.0
9	1.0	2.0	2.0
10	1.0	1.0	2.0
11	0.75	1.0	1.5
12	0.75	2.0	1.5
13	0.75	3.0	1.5

[1]Spacing is from centre to centre leaving 0.25 mm groove separation.

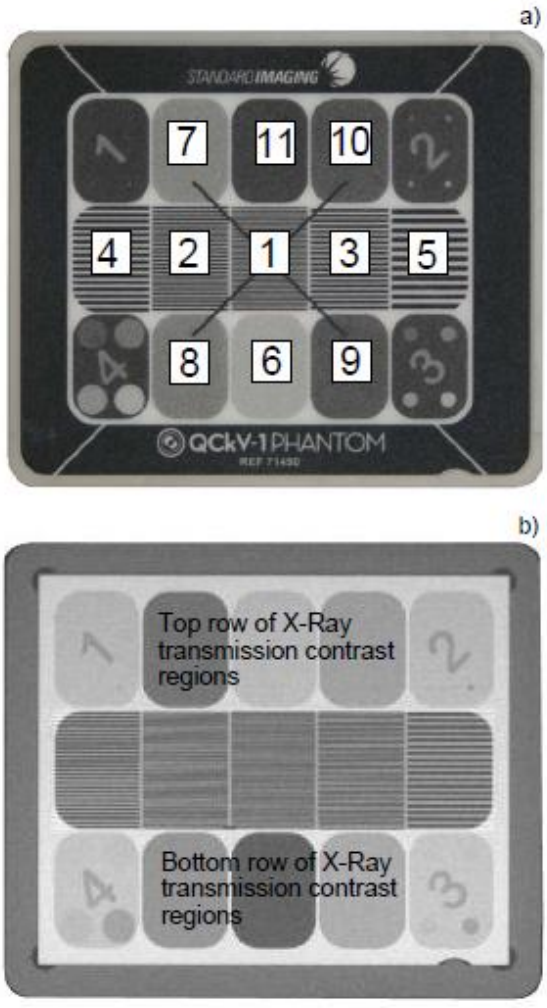

Figure 5. Photograph (a) and x-ray image (b) of the image quality test phantom. The regions of interest are numbered 6-11 in the white text boxes.

Table 2. Properties of commercial phantom

Region	Bar resolution (lp/mm)	Bar thickness (inches)
1	2.46	3.0
2	2.00	6.0
3	1.50	3.0
4	0.98	6.0
5	0.66	9.0
	Transmission Rate at 80 kV	
6	10%	
7	20%	
8	30%	
9	40%	
10	40%	
11	50%	

The consistency of the x-ray formation is assessed using the upper and bottom contrast regions of Figure 5 b). The pixel intensity variation for 9 sessions over 70 days is plotted in Figure 6. It is evident that there is a non-uniform change in pixel intensity between the contrast regions. Since the transmission over the 5 regions is increasing by 10% increments from 10% to 50%, the change in pixel intensity between each incrementally higher transmission region should be linear. Unfortunately, as shown in Figure 6, this is currently not the case, which indicates that the x-ray transmission is not being mapped to the ideal pixel intensity value. This will affect the linearity in the display of contrast and thus hinder the results of the correct cracking pattern. The pixel intensity for each region should also be constant over all nine imaging sessions. A variation in intensity, possibly resulting from drift in the calibration of the kV imager, will cause discrepancies in the contrast between consecutive images. This intensity variation has to be corrected in order to accurately predict the cracking patterns of a GCL.

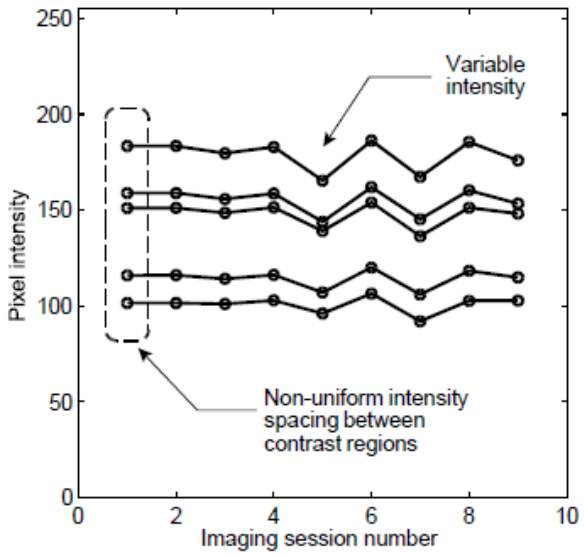

Figure 6. Variation in pixel intensity for contrast regions 6-9 and 11 over nine imaging sessions on different days.

To investigate the potential causes of these x-ray transmission mapping errors to pixel intensity, the x-ray images of the commercial phantom were investigated in more detail. Figure 7 represents the location on the Bar Phantom where the minimum transmission (white reference) and 100% transmission (black reference) occur. These two points are the reference points for the whitest and darkest intensities on the phantom x-ray.

By visual inspection it is apparent that there is a slight change in pixel intensity from the top row of the x-ray transmission contrast regions to the bottom row. Section A-A' in Figure 7 is inspected by plotting the variation in intensity across this segment and is shown in Figure 8. This data confirms that there is a variation in the pixel intensity of white from point A to A' (white reference). The minimum white pixel intensity is approximately 197 and increases along this section to a maximum intensity of approximately 230. Since the pixel intensity of this constant contrast region varies with vertical position in the image, this variation will cause a non-linear spacing of the contrast regions 6-11 as regions of increasing transmission are alternatively located on the top and bottom row of contrast regions.

A strategy for the correction for the observed variation in pixel intensity of the constant contrast regions was adopted in which four regions were selected in the image to capture the variation in pixel intensity for maximum transmission of x-rays (black reference) and for the minimum transmission (white reference). These four regions were located in the corners of the image and the variation observed in black and white references were modelled with a linear variation along both the horizontal and vertical extents of the image.

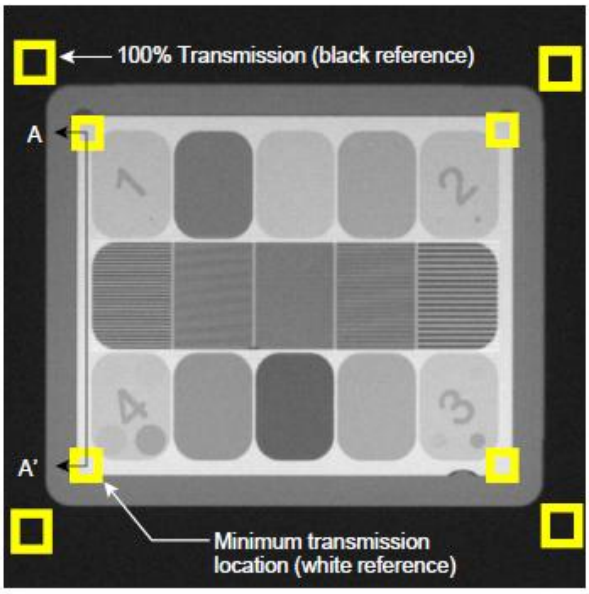

Figure 7. Bar Phantom indicating location of minimum and maximum transmission.

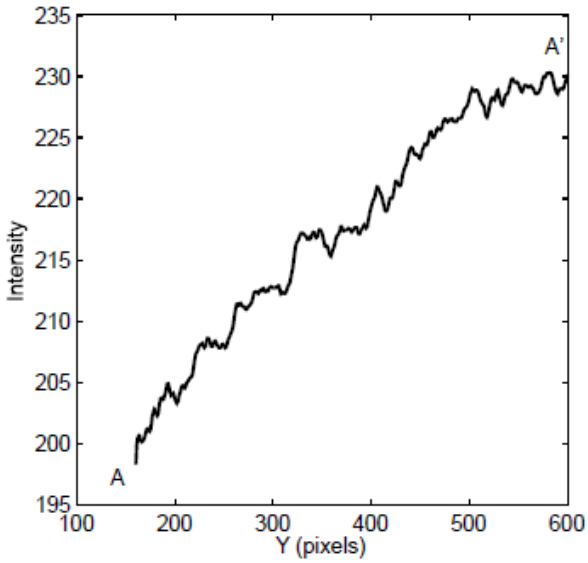

Figure 8. Variation in pixel intensity of white across the section A-A' of the Bar Phantom.

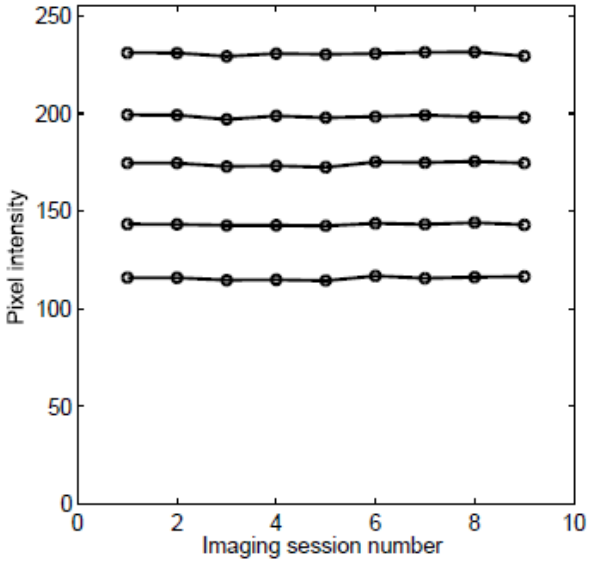

Figure 9. Variation in corrected pixel intensity for five contrast regions over nine imaging sessions on different days

A normalised intensity, $i_{n,}$ at a location in the image (x,y) was then defined as

$$i_n = ((i(x,y) - i_b(x,y))/(i_w(x,y) - i_b(x,y))\cdot(i_{max}) + i_b(x,y) \quad [1]$$

where the current pixel intensity at a location (x,y) is i(x,y), and the intensity of the linear fit to the variation of black and white reference at this location are $i_b(x,y)$ and $i_w(x,y)$ respectively. The maximum pixel intensity (i_{max}) was then set at a value of 230 which was chosen to be slightly below pure white (pixel intensity 255) to increase the contrast of the image. Once this correction was applied, the variation in pixel intensity of each contrast region was plotted against image session number in Figure 9. This data indicates that the normalised pixel intensity calculation of Equation 1 is an effective approach to remove the non-uniform intensity spacing between incrementally higher contrast regions and the variable intensity of contrast regions between x-ray sessions.

The same approach was applied to each GCL x-ray image in order to correct the similar issues that occurred between imaging sessions. For the GCL x-ray images, the bottom left corner washer acts as the minimum transmission location (white reference) and the 100% transmission (black reference) occurs at the four corners as shown in Figure 10. Using the similar correction techniques applied to the commercial phantom, the impact of the small contrast between the cracked areas and the bentonite regions can be overcome.

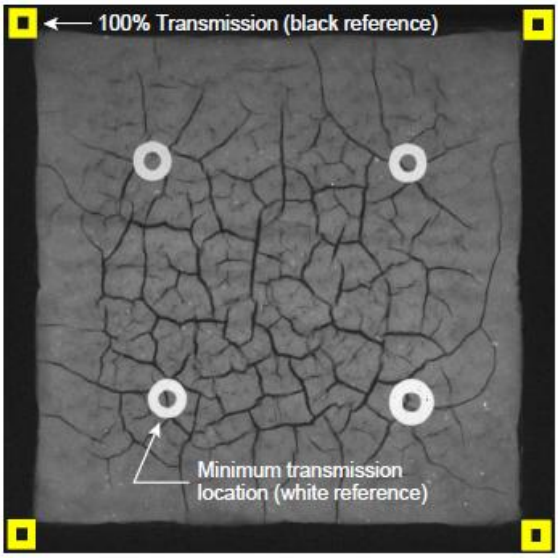

Figure 10. Location of the white and black reference locations in x-ray images of GCL cracking

5 OBSERVED EVOLUTION OF CRACK PATTERNS

The processed x-ray images of the GCL specimen captured gravimetric moisture contents of 198.0%, 124.3%, and 9.6% are shown in Figure 11. These images indicate that at full saturation, no visible cracks exist in the GCL sample, but as moisture is withdrawn from the specimen small cracks are formed (Figure 11b).

Figure 11. Desiccation cracks developed in the GCL specimen at a gravimetric water content of a) 198% b) 124.3% and c) 9.6%.

It is interesting to note that the restrain of the shrinkage strains by the needle punched geosynthetic results in cracking at high moisture contents as high as 124.3%, as shown by Figure 11b. Further drying causes these original cracks to grow in width and new cracks to form between the original cracks to further segment the bentonite (Figure 11c). Also visible in the image is the shrinkage of the GCL specimen by comparing the size of the initial saturated (Figure 11a) sample and the final air-dry cracked sample (Figure 11c).

The ability of x-ray imaging to non-destructively capture the cracking process in GCLs is a significant experimental tool as it now permits experiments to be conducted to investigate the suction required for GCL samples to crack on a drying curve as well as the suction required for GCL samples to self-heal through crack closure on a wetting curve. Both of these experiments are a subject of current ongoing research.Although the presence of the moisture barrier tape is helpful in eliminating the loss of bentonite from the edges of the specimen during handling (e.g. it is essential for enabling the accurate tracking of moisture content during drying), the moisture barrier tape led to a small region around the periphery of the specimen to temporarily experience less cracking than the centre of the specimen. However, by the time the GCL reached the lowest moisture content tested (9.6%), this effect of the tape was no longer visually evident. These observations indicate that future specimens should use a reduced width of tape located at the edge of the specimen.

6 CONCLUSIONS

X-ray imaging has proven to be an effective non-destructive imaging technique to monitor the desiccation cracking of GCLs. An analysis of a commercial phantom consisting of linearly varying pixel intensity regions has enabled a correction to be made for small variations in pixel intensity with spatial location in the image or with temporal variations in the imager calibration. These techniques have proven to be effective in capturing the pattern of desiccation cracks in a GCL test specimen. This preliminary study indicates that, although the bentonite in GCLs is only approximately 1 cm thick and has a relatively low material density, the corrected images can adequately capture the evolution of cracking in a GCL specimen. This indicates that this technique could be used to develop a relationship between the cracked area of a GCL and the GCL's gravimetric moisture content. Such a relationship could be used to investigate the matric suction required for different GCL products to initiate cracking upon moisture loss. Further experimental work is currently being undertaken to collect the data required to formulate this relationship. This work is currently ongoing.

ACKNOWLEDGEMENTS

This study was financially supported by the Natural Science and Engineering Research Council of Canada (NSERC)

REFERENCES

Albrecht, B.A and Benson, C.H. 2001. Effect of desiccation on compacted natural clays. *Journal of Geotechnical and Geoenvironmental Engineering*, 127: 67-75.

Beddoe, R. A., Take, W. A. and Rowe, R. K. 2010. Development of suction measurement techniques to quantify the water retention behaviour of GCLs. *Geosynthetics International*, 17, No. 5, 301–312. [doi: 10.1680/gein.2010.17.5.301]

Beddoe, R.A., Take, W.A. and Rowe, R.K. 2011. Water retention behaviour of geosynthetic clay liners. *Journal of Geotechnical and Geoenvironmental Engineering,* ASCE, doi:10.1061/(ASCE)GT.1943-5606.0000526

Boardman, B.T and Daniel, D.E. 1996. Hydraulic conductivity of desiccated geosynthetic clay liners. *Journal of Geotechnical Engineering*, 122: 204-208.

Bostwick, L., Rowe, R. K., Take, W. A. and Brachman, R.W.I. 2010. Anisotropy and directional shrinkage of geosynthetic clay liners. *Geosynthetics International* 17: 157–170. [doi: 10.1680/gein.2010.17.3.157]

Brachman, R. W. I., Rowe, R. K., Take, W. A., Arnepalli, D. N., Chappel, M., Bostwick, L. E. and Beddoe, R. A. 2007. *Queen's composite geosynthetic liner experimental site*., Ottawa. :2135-2142.

Huda, W. 2009. *Review of radiologic physics*. 3rd ed., Lippincott Williams & Wilkins, Baltimore, MD, USA.

Koerner, R.M. and Koerner, G.R. 1995. Temperature Behavior of Field Deployed HDPE Geomembranes, *Geosynthetics '95*, IFAI, Nashville, TN, USA, 3:921-937.

Koerner, R.M. and Koerner, G.R. 2005. InSitu separation of GCL panels beneath exposed geomembranes, *Geotechnical Fabrics Report,* June-July 2005: 34-39.

Rowe, R.K., Bostwick, L.E., and Take, W.A. 2011. Effect of GCL properties on shrinkage when subjected to Wet-Dry Cycles, ASCE Journal of Geotechnical and Geoenvironmental Engineering, published online first, doi:10.1061/(ASCE)GT.1943-5606.0000522

Standard Imaging Inc. 2011. *QCkV-1 Phantom User Manual.* Standard Imaging Inc., Middleton, WT, USA. <www.standardimaging.com>

Take, W.A., Rowe, R.K., Munro, H., Kerr, A., Schreiner, J. 2009. Development of X-ray imaging techniques to investigate the internal shrinkage mechanism of GCLs. *Geosynthetics '09*, Salt Lake City, UT, USA

Thiel, R. and Richardson, G. 2005. Concern for GCL shrinkage when installed on slopes, *JGRI-18 at GeoFrontiers*, GII Publications, Folsom, PA, USA,